Journal of Inorganic Biochemistry 265 (2025) 112819

Contents lists available at ScienceDirect

Journal of Inorganic Biochemistry

journal homepage: www.elsevier.com/locate/jinorgbio

Ruthenium(II)-mercapto complexes induce cell damage *via* apoptosis pathway on ovarian cancer cells

Marcos V. Palmeira-Mello [a,*], Tamara Teixeira [a], Matheus Reis Santos de Melo [b], Heloiza Diniz Nicolella [a,b], Jocely L. Dutra [a], Marcia R. Cominetti [c], Fillipe Vieira Rocha [a], Denise Crispim Tavares [b], Alzir A. Batista [a,*]

[a] Departament of Chemistry, Universidade Federal de São Carlos (UFSCar), 13561-905 São Carlos, SP, Brazil
[b] Laboratory of Mutagenesis, Universidade de Franca, 14404-600 Franca, SP, Brazil
[c] Departamenty of Gerontology, Universidade Federal de São Carlos (UFSCar), 13565-905 São Carlos, SP, Brazil

ARTICLE INFO

Keywords:
3D tumor spheroids
Apoptosis
Bioinorganic chemistry
Mitochondrial damage
Ovarian cancer
Ruthenium(II)-phosphine complex

ABSTRACT

Ovarian cancer represents a leading cause of cancer-related deaths in women worldwide. Chemotherapeutic agents are usually employed to treat the patients, and Ruthenium(II)-based compounds have been investigated as possible substitutes for platinum drugs. In this work, we studied three different Ru(II)-phosphine-mercapto complexes (**1–3**) as potential cytotoxic agents against A2780 and A2780-*cis*R ovarian cancer cells. A time-dependent cytotoxicity was observed for **2**, which also exhibited better selectivity than cisplatin control. A similar cytotoxic behavior was observed on 3D tumor spheroids. Although no changes were observed in cell cycle distribution, compound **2** affected the mitochondrial membrane potential on A2780 cells, and caused cell death *via* apoptotic pathway, which was confirmed by flow cytometry assay. Western blotting experiments revealed that **2** affected the expression of p53, PCNA, γH2AX and cleaved caspase-3, making it a promising anticancer agent for ovarian cancer.

1. Introduction

Ovarian cancer (OC) is one of the most common cancers of the female reproductive system and the leading cause of cancer-related deaths in women worldwide. It can be distinguished into different types, and epithelial ovarian carcinomas (EOCs) are identified in about 90 % of women diagnosed with the disease [1]. In addition to surgery, treating this disease involves different strategies such as chemo, radio, hormone, targeted, and immunotherapies, which can be employed isolated or in combination. Regarding chemotherapy [2], as the first treatment, a combination of cisplatin/carboplatin and paclitaxel or docetaxel is indicated for ovarian cancer however, its efficacy is limited due to drug resistance. Cisplatin and carboplatin bind to DNA forming platinum adducts, thus inhibiting both replication and transcription processes [3,4]. Mostly, the resistance to platinum-based drugs comes from the failure of DNA repair process, which is activated after structural alterations in the double helix [5]. Additionally, the resistance in ovarian cancer cells involves several biological tasks such as cell metabolism, oxidative stress, cell cycle regulation, and apoptosis [6,7]. Therefore, new strategies to overcome this issue are urgently needed.

Several metal complexes have been extensively investigated as possible anticancer agents and Ru-based compounds are considered a promising alternative to platinum drugs [8–13]. Although the success of NAMI-A, KP1019, and KP1339, no one ruthenium complex presented the requirements to reach the marketplace until nowadays [14,15]. Thus, efforts have been made in our group to obtain new Ru(II)-based phosphine complexes as possible chemotherapeutic agents. These compounds have gained attention in the medicinal chemistry field due

Abbreviations: 7-AAD, 7-Aminoactinomycin D; ATP, adenosine triphosphate; bipy, 2,2′-bipyridine; DAPI, 4′,6-diamidino-2-phenylindole; DMEM, Dulbecco's modified Eagle's medium; dppb, 1,4-bis(diphenylphosphino)butane; dppe, 1,2-bis(diphenylphosphino)ethane; EOCs, epithelial ovarian carcinomas; Hdmp, 4,6-diamino-2-mercaptopyrimidine; Hmmi, mercapto-1-methylimidazole; Hmtz, 1,3-thiazolidine-2-thione; MCTS, multicellular tumor spheroids; MMP, mitochondrial membrane potential; MTT, 3-(4,5-dimethylthiazol-2-yl)-2,5-diphenyltetrazolium bromide; OC, ovarian cancer; OXPHOS, oxidative phosphorylation; PI, propidium iodide; PS, phospholipid phosphatidylserine; PVDF, polyvinylidene fluoride; RPMI 1640, Roswell Park Memorial Institute 1640 medium; SI, selectivity index.

* Corresponding authors.
E-mail addresses: marcos.palmeira@ufscar.br (M.V. Palmeira-Mello), daab@ufscar.br (A.A. Batista).

https://doi.org/10.1016/j.jinorgbio.2024.112819
Received 26 August 2024; Received in revised form 27 November 2024; Accepted 26 December 2024
Available online 30 December 2024

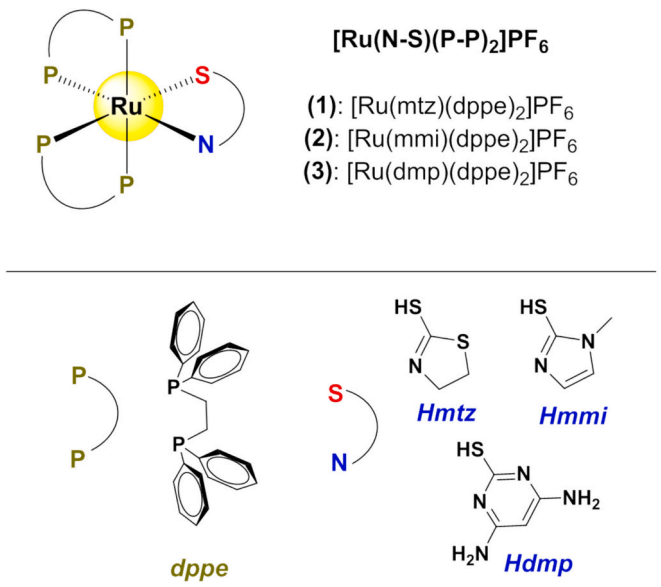

Fig. 1. Chemical structures of ruthenium(II) compounds (**1**–**3**). dppe = 1,2-bis (diphenylphosphino)ethane, and Hmtz = 1,3-thiazolidine-2-thione, Hmmi = mercapto-1-methylimidazole, and Hdmp = 4,6-diamino-2-mercaptopyrimidine.

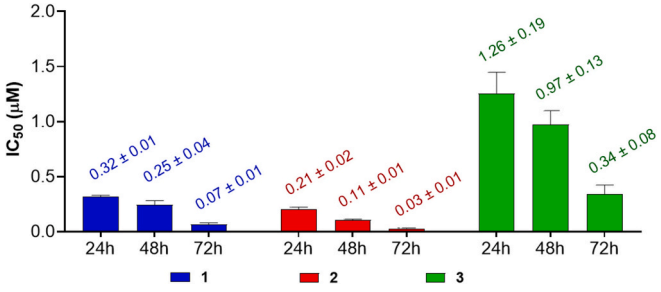

Fig. 2. Cytotoxicity activity of compounds **1–3** on A2780 cells after 24, 48 and 72 h. Data are presented as mean ± SD of three independent replicates.

to their increased cytotoxicity against different cancer cell lines [16–22] and their ability to interact with several biological targets, such as DNA and mitochondria. These cellular organelles are present in most eukaryotic cells and play a crucial role in cellular metabolism *via* oxidative phosphorylation (OXPHOS) to produce adenosine triphosphate (ATP). Moreover, recent studies revealed that Ru(II)-phosphine complexes can induce mitochondrial dysfunction in different cancer cells, revealing apoptosis *via* mitochondrial damage as a possible mechanism of action [23,24]. Despite these promising results, to the best of our knowledge, studies involving Ru(II)-phosphine compounds as potential chemotherapeutic agents for ovarian cancer cells are limited, and there is a lack of deeper biological investigations on the theme.

Here we investigate the *in vitro* anticancer profile of three ruthenium compounds with the general formula $[Ru(N—S)(dppe)_2]PF_6$ {dppe = 1,2-*bis*(diphenylphosphino)ethane and N–S = 1,3-thiazolidine-2-thione (**1**, mtz), mercapto-1-methylimidazole (**2**, mmi) or 4,6-diamino-2-mercaptopyrimidine (**3**, dmp) in their deprotonated forms} against A2780 (Human Ovarian Carcinoma) and A2780-*cis*R (Human Ovarian Carcinoma Cisplatin Resistant) (Fig. 1). Compound **2** $[Ru(mmi)(dppe)_2]PF_6$ was further studied to obtain a deeper understanding of its biological profile. Morphological and clonogenic experiments were also performed. We demonstrate that **2** causes disruption of mitochondrial membrane potential (MMP) and induces cell death *via* apoptosis without affecting cell cycle distribution on A2780 ovarian cancer cells.

2. Experimental section

2.1. Synthesis and characterization

All Ruthenium compounds (**1**–**3**) have been previously reported [25]. In a Schlenk flask with a mixture of 15 mL of methanol and 15 mL of CH_2Cl_2 previously degassed, 0.12 mmol of the respective mercapto ligand was added along with 32 μL (24 mmol) of triethylamine. Posteriorly, 0.10 mmol (0.097 g) of the precursor *cis*-$[RuCl_2(dppe)_2]$ and 0.13 mmol (0.024 g) of KPF_6 were added to the flask. The system was kept under stirring and reflux for approximately 12 h. The volume of the solution was reduced to about 2 mL and water was added to precipitate a yellow powder. The precipitate was filtered off, washed with water and ethyl ether, and dried under vacuum. ^{31}P NMR spectra were recorded on a Bruker DRX 400 MHz using CH_2Cl_2/D_2O. Elemental analyses were performed in the Microanalytical Laboratory at the Universidade Federal de São Carlos, São Carlos, Brazil, with an EA 1108 CHNS microanalyzer (Fisons Instruments). Mass spectrometry analyses were performed using an Agilent 6545 ESI-QTOF-MS instrument. The target MS/MS data were produced across the mass range of 50–1200 Da. Samples were dissolved in MeOH/0.1 % formic acid and analyzed by FIA in a flow rate of 0.35 mL min^{-1} and volume injection of 2.0 μL at 38 °C. The mobile phase consisted of H_2O + 0.1 % formic acid and MeOH +0.1 % formic acid (20:80) with 4.0 min of analysis time.

2.2. Biological investigation

2.2.1. Cell culture

The ruthenium compounds (**1**–**3**) were tested against human ovarian cancer cells A2780 (ECACC 93112519), cisplatin-resistant human ovarian cancer cells A2780-*cisR* (ECACC 93112517) and non-cancerous lung cells MRC-5 (ATCC CCL-171). The cells were routinely maintained with Roswell Park Memorial Institute 1640 medium (RPMI 1640, for A2780 and A2780-*cisR*) or Dulbecco's modified Eagle's medium (DMEM, for MRC-5) supplemented with 10 % fetal bovine serum (FBS), at 37 °C in a humidified 5 % CO_2 atmosphere. The cells were obtained from Rio de Janeiro Cell Bank (BCRJ). Cell culture media and FBS were obtained from Vitrocell and Gibco, respectively.

2.2.2. In vitro cytotoxicity

The cytotoxic activity of the complexes was investigated *via* 3-(4,5-dimethylthiazol-2-yl)-2,5-diphenyltetrazolium bromide (MTT) assay [26]. Cells were seeded in 96-well plates (150 μL/well) and incubated for 24 h (37 °C, 5 % CO_2).

After this period, 0.75 μL of the compounds were added at 8 different concentrations (0.012 to 30 μmol L^{-1}), containing a final concentration of 0.5 % DMSO, and the plates were kept in the incubator for 24, 48 or 72 h. After the incubation, 50 μL of MTT (1.0 mg mL^{-1} in PBS) was added to each well and the cells were incubated again for 4 h. After that, the medium was removed, and the formazan crystals formed were solubilized by adding 150 μL of isopropyl alcohol. The absorbance was measured using a microplate spectrophotometer (BioTek™, Epoch™) at 540 nm. All compounds were tested in three independent experiments performed in triplicate. Cisplatin drug was also tested as the positive control and DMSO was used as the negative control (0.5 %). From the absorbance, IC_{50} (concentration required to inhibit cell viability by 50 %) was calculated using GraphPad Prism 8.0 software and reported as mean ± standard deviation.

2.2.3. Morphological changes

Cells (0.6×10^5 cells/well) were seeded in a 12-well plate and after 24 h were treated with different concentrations of **2** for an additional 48 h (0.5 × IC_{50}, IC_{50}, 2 × IC_{50} and 4 × IC_{50} concentrations based on cytotoxicity results for 48 h). Cells were examined at 0, 24, and 48 h under an inverted optical microscope (NIKON ECLIPSE TS100) with a 10 × objective lens, coupled with a Motcam 1SP camera. DMSO was

used as the negative control (0.5 %). The morphological changes of the cells exposed to the treatment were compared to those of the negative control.

2.2.4. Clonogenic assay

A total of 500 cells were cultured per well in a 6-well plate. After 24 h, **2** was added at different concentrations (0.5 × IC_{50}, IC_{50}, 2 × IC_{50} and 4 × IC_{50} concentrations based on cytotoxicity results for 48 h). The plates were incubated (37 °C, 5 % CO_2) during 48 h. Then, the culture medium was replaced by a fresh medium and the plates were incubated for an additional 10 days. After this period, the culture medium was removed, and the wells were washed with PBS. The colonies formed were fixed with a methanol/acetic acid (3:1) solution (30 min), and then colored with violet crystal 0.5 % (30 min). Further, the plates were washed with water and dried. The images were taken using an Invitrogen iBright 1500 Imaging System (Thermofisher). The test was performed in triplicate and DMSO was used as the negative control (0.5 %). Relative survival was calculated using ImageJ software using the *"Colony Area"* Plug-in and the *"Watershed"* and *"Analyze Particles"* functions. The parameters size (0.01-infinity) and circularity (0.30–1.00) were employed.

2.2.5. MCTS growth inhibition

For the multicellular tumor spheroids (MCTS) culture, the Bioprint Kit from Magnetic 3D Cell Culture Technology m3D-Greiner (Greiner Bio-One, Frickenhausen, Germany) was used. In a 25 cm^2 bottom containing A2780 cells, was added 150 μL of nanoparticle solution (NanoShuttle - PL) for the magnetization. After 24 h, the cells were trypsinized, counted and seeded in a 96-well plate (1.5 × 10^3 cells/well). The plate was used in a magnetic drive to obtain the spheroids and incubate at 37 °C and 5 % CO_2. The growth was observed using a microscope CELENA® S Digital Imaging System (Logos Biosystems). After this period, compound **2** was added at different concentrations (0.1, 0.4, 1.0, 6.25 and 10 μM) and incubated for 6 days. After the last day, 4′,6-diamidino-2-phenylindole (DAPI) and propidium iodide (PI) were added and the images were taken using a CELENA® S Digital Imaging System (Logos Biosystems). The diameters of the spheroids were analyzed using ImageJ software and treated statistically in GraphPad Prism 8.0.

2.2.6. Cell cycle analysis

The distribution of cell cycle was investigated by flow cytometry. A2780 cells (1.0 × 10^5 cells/well) were seeded in a 12-well plate and incubated (37 °C, 5 % CO_2) for 24 h. After this period, **2** was added at different concentrations (0.5 × IC_{50}, IC_{50} and 2 × IC_{50} concentrations based on cytotoxicity results for 48 h) and the cells incubated for an additional 24 h. Subsequently, the cells were collected with a scraper, washed with ice-cold PBS, and fixed in 70 % ethanol at −20 °C for 24 h. After fixation, the cells were centrifuged at 2000 rpm and 4 °C for 10 min, resuspended in 250 μL of PBS buffer containing RNAse A (0.2 mg mL^{-1}) and PI (Propidium Iodide, 5 μg mL^{-1}), and incubated for 30 min on ice and in the dark. The DNA contents were analyzed on an Accuri C6 (BD Biosciences) flow cytometer;; 10 000 events were recorded. The cell cycle phase distribution was analyzed in triplicate by using the FlowJo Software. Treated cells with DMSO (0.5 %) were the negative control.

2.2.7. Mitochondria membrane potential test

A2780 cells were seeded at a density of 1.0 × 10^4 cells/well in black 96-well plates (Corning) and maintained at 37 °C in a 5 % CO_2 atmosphere for 24 h. Cells were treated with different concentrations of **2** (0.01–5 μM) and incubated for an additional 24 h. After this period, the medium was removed and treated with a JC-1 solution (100 μL, culture medium without phenol red) and maintained at 37 °C in a 5 % CO_2 atmosphere for 30 min. After incubation, the cells were washed with PBS, the fluorescence signal of JC-1 was read using a Synergy/H1-Biotek fluorometer (aggregate, Ex/Em: 535/590 nm and monomer, Ex/Em: 475/530 nm), and the images were taken using a CELENA® S Digital Imaging System (Logos Biosystems). The data were analyzed using GraphPad Prism 8 software.

2.2.8. Apoptosis assay

The programmed cell death was evaluated by flow cytometry using an annexin-V-PE Apoptosis Detection Kit (BC Biosciences). A2780 cells (1.0 × 10^5 cells/well) were seeded in a 12-well plate and incubated (37 °C, 5 % CO_2) for 24 h. Then, the cells were exposed to increasing concentrations (0.5 × IC_{50}, IC_{50}, 2 × IC_{50} and 4 × IC_{50} concentrations based on cytotoxicity results for 48 h) of **2** for 24 h. After treatment, the medium was removed, 150 μL of binding buffer was added to each well, PE-Annexin V (2.5 μL) and 7ADD (2.5 μL) were added, which was followed by incubation in the dark at room temperature for 20 min. Then, under ice, the cells were collected with a scraper, centrifuged at 1000 rpm and 4 °C for 5 min, the supernatant removed, resuspended in 200 μL of binding buffer, and analyzed on an Accuri C6 (BD Biosciences) flow cytometer; 10 000 events were recorded. Cell samples were analyzed in an Accuri C6 flow cytometer (BD Biosciences) using FL2 and FL3 channels. DMSO (0.5 %) was used as the negative control and the experiment was performed in triplicate.

2.2.9. DAPI/PI staining

Cells (0.7 × 10^5 cells/well) were seeded in a 12-well plate and after 24 h, were exposed to **2** (2 × IC_{50}) for an additional 48 h. Then, the cells were incubated with 4′,6-diamidino-2-phenylindole (DAPI) and propidium iodide (PI) for 1 h and the images were taken using a CELENA® S Digital Imaging System (Logos Biosystems).

2.2.10. Western blotting

The effect of compound **2** on some molecular signaling pathways was studied using Western blot assay. In this sense, its action on genomic stability, cell proliferation, capacity to induce DNA damage and apoptosis was evaluated through the expression of the proteins p53, PCNA, γH2AX and cleaved caspase-3, respectively. The A2780 cells were treated with the **2** at concentrations of IC_{50} and 2 x IC_{50} for 24 h. Experimental procedures were conducted as described by Ribeiro et al. [27] Cells were lysed using RIPA buffer supplemented with phosphatase and protease inhibitors (Sigma-Aldrich). Protein concentrations were measured using the BCA assay (Thermo Scientific, Waltham, Massachusetts, USA). Protein extracts (120 μg) were loaded onto a 12 % polyacrylamide gel (SDS-PAGE) and separated by electrophoresis, followed by transfer to a polyvinylidene fluoride (PVDF) membrane (Bio-Rad Laboratories, Hercules, California, USA). The PVDF membrane was blocked for 2 h in Tris-buffered saline with 0.1 % Tween (TBST, Bio-Rad Laboratories) containing 5 % of non-fat dry milk.

After blocking step, the membrane was incubated overnight at 4 °C with the primary antibodies: p53 (DO-1) (Santa Cruz Biotechnology, Dallas, Texas, USA; 126), PCNA (D3H8P) (Cell Signaling, Danvers, Massachusetts, USA;13110S), phosphorylated histone γH2AX (Ser 139) (Santa Cruz Biotechnology, Dallas, Texas, USA; sc-517348), and cleaved caspase-3 (Asp 175) (Cell Signaling; # 9661). The anti-beta actin antibody was used as the loading control (Cell Signaling; 13E5).

The membrane was subsequently incubated for 1 h at room temperature with secondary antibodies (anti-mouse m-IgGκ BP-HRP - Santa Cruz Biotechnology - 516102; and anti-rabbit IgG-HRP - Li-Cor - 926-80011). The protein bands were detected using Immobilon Western Chemiluminescent HRP Substrate reagent (Merck). The intensity, absolute area, and relative percentage of area of band were determined using the ImageJ software.

The results were expressed as the ratio between the relative percentage of the band area of the target antibody (p53, PCNA, γH2AX, and/or cleaved caspase-3) and the relative percentage of the band area of the β-actin antibody (loading control), according to the following formula:

Table 1
In vitro cytotoxicity (IC_{50}, μM) results against A2780 and A2780-*cis* ovarian cancer cells, and non-cancerous lung cells MRC-5 after 48 h of incubation. Data are presented as mean ± SD of three independent replicates. Hmtz: 1,3-thiazolidine-2-thione, Hmmi: mercapto-1-methylimidazole and Hdmp: 4,6-diamino-2-mercaptopyrimidine. SI1 = IC_{50} MRC-5/IC_{50} A2780; SI2 = IC_{50} MRC-5/IC_{50} A2780-*cis*.

Complex	A2780	A2780-*cisR*	MRC-5	SI1	SI2
1	0.25 ± 0.04	0.19 ± 0.05	1.11 ± 0.09	4.44	5.84
2	0.11 ± 0.01	0.12 ± 0.08	0.71 ± 0.12	6.45	5.92
3	0.97 ± 0.13	1.49 ± 0.31	1.22 ± 0.15	1.26	0.82
Hmtz	> 100	> 100	> 100	–	–
Hmmi	> 100	> 100	> 100	–	–
Hdmp	> 100	> 100	> 100	–	–
$[RuCl_2(dppe)_2]$	0.93 ± 0.01	0.94 ± 0.22	2.83 ± 0.06	3.04	3.04
Cisplatin	8.73 ± 0.45	37.02 ± 5.10	29.09 ± 0.79	3.33	0.79

$$Ratio = \left(\frac{R.P.(\ antibody\ of\ interest)}{R.P.\beta - Actin}\right)$$

The data obtained were statistically analyzed using analysis of variance (ANOVA) for completely randomized experiments, with the calculation of the F-statistic and its respective *p*-value. In cases where $p < 0.05$, Tukey's test was used to calculate the minimum statistical difference for $p = 0.05$. Statistical analysis was performed using GraphPad Prism 8 software.

3. Results and discussion

3.1. Synthesis and characterization

The reaction between the precursor $[RuCl_2(dppe)_2]$ and the respective mercapto ligands (N—S) in the presence of Et_3N provides the complexes **1**–**3**. These compounds were characterized by ^{31}P NMR and mass spectrometry, and their purity confirmed by elemental analyses (See Supplementary Information) [25]. $^{31}P\{^1H\}$ NMR experiments confirmed their stability in DMSO during 48 h, as reported by Silva and co-workers [25]. After characterizing the Ru(II) compounds, these same samples were used for the biological experiments.

3.2. In vitro cytotoxicity

The cytotoxicity of compounds **1**–**3** was investigated on A2780 and A2780-*cis*R ovarian cancer and MRC-5 non-cancerous lung cells using MTT assay. In general, all compounds presented better performance against A2780 cells in comparison to the resistant lineage and were more cytotoxic than cisplatin control (Table 1). These Ruthenium complexes were also cytotoxic on MRC-5 non-cancerous cells, exhibiting IC_{50} values from 0.71 to 1.22 μM. Although our results revealed **2** as the most cytotoxic compound on ovarian cells, we should highlight the similar behavior for **1** in different cancer cell lines, such as A549 (lung) and MDA-MB-231 (breast) [25]. Analogous compounds, such as Ru(mtz)(dppb)(bipy)]PF_6 and Ru(mmi)(dppb)(bipy)]PF_6 were cytotoxic on these cell lines, exhibiting lower IC_{50} values around 0.11–0.22 μM (bipy = 2,2′-bipyridine and dppb = 1,4-bis(diphenylphosphino)butane) [28]. As observed, the free mercapto ligands had no activity at the maximum concentration tested (100 μM).

In a next step, we were able to assess the selectivity index (SI) for these compounds. The results revealed **2** as the most promising compound, exhibiting the best SI index on A2780 cells. It should be highlighted that **2** was found as more selective than **1** and **3**, and 2-fold more selective than cisplatin drug.

To verify the time-dependent cytotoxicity of the complexes we evaluate their activities after 24 h and 72 h of incubation (Fig. 2). The results revealed that the incubation-time effect cause slightly changes on cytotoxicity* of **1** and **2**. For example, the IC_{50} values goes from 0.32 to 0.07 μM (for **1**) and from 0.21 to 0.03 μM (for **2**). Although **3** presented the lowest cytotoxicity, the incubation time revealed a remarkable change in its IC_{50}, which goes from 1.26 to 0.34 μM (almost 4 times increased activity). This behavior was previously reported for other metal-based compounds in ovarian cancer cells [29,30].

3.3. Morphological and clonogenic assays

The morphology of ovarian A2780 cancer cells was studied after exposition to compound **2** during 48 h. Alterations in the shape of the cells were observed, and non-adherent and spherical cells were found, mainly after 24 h of treatment at concentrations higher than IC_{50}, which are typical marker of cell death (Fig. 3) [31]. Upon verifying morphological alterations on A2780 cells, a clonogenic assay was performed to study how **2** affected the colony formation in this cell line [32] (Fig. 4).

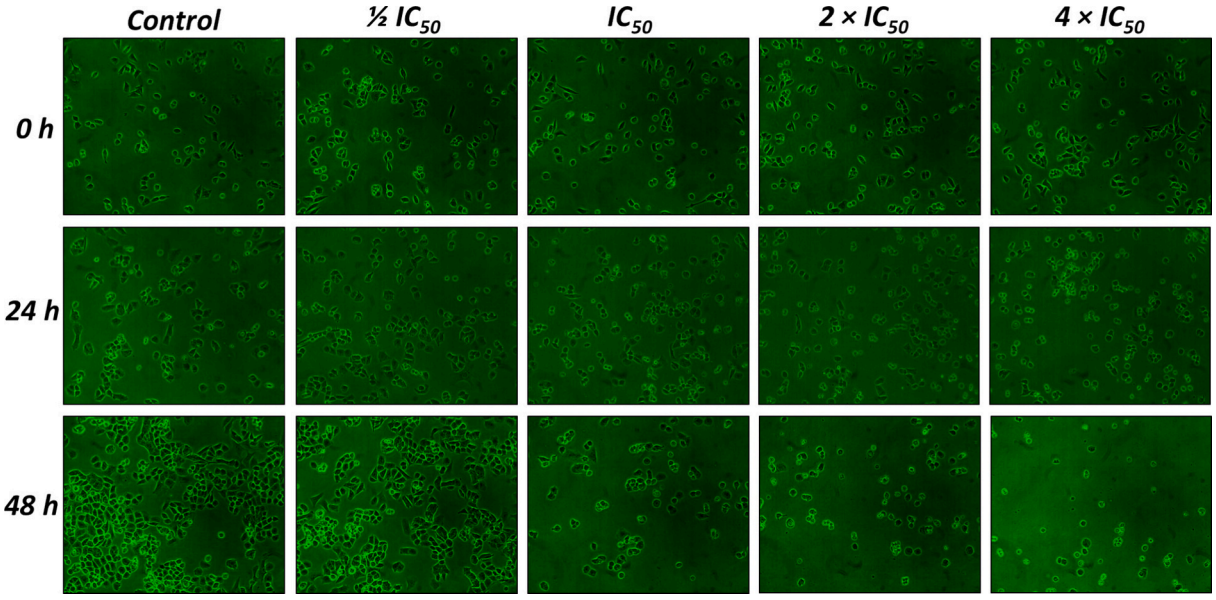

Fig. 3. Microscopy images showing the cellular morphology of A2780 cells after 48 h treatment with different concentrations of **2**. DMSO was used as negative control (0.5 %).

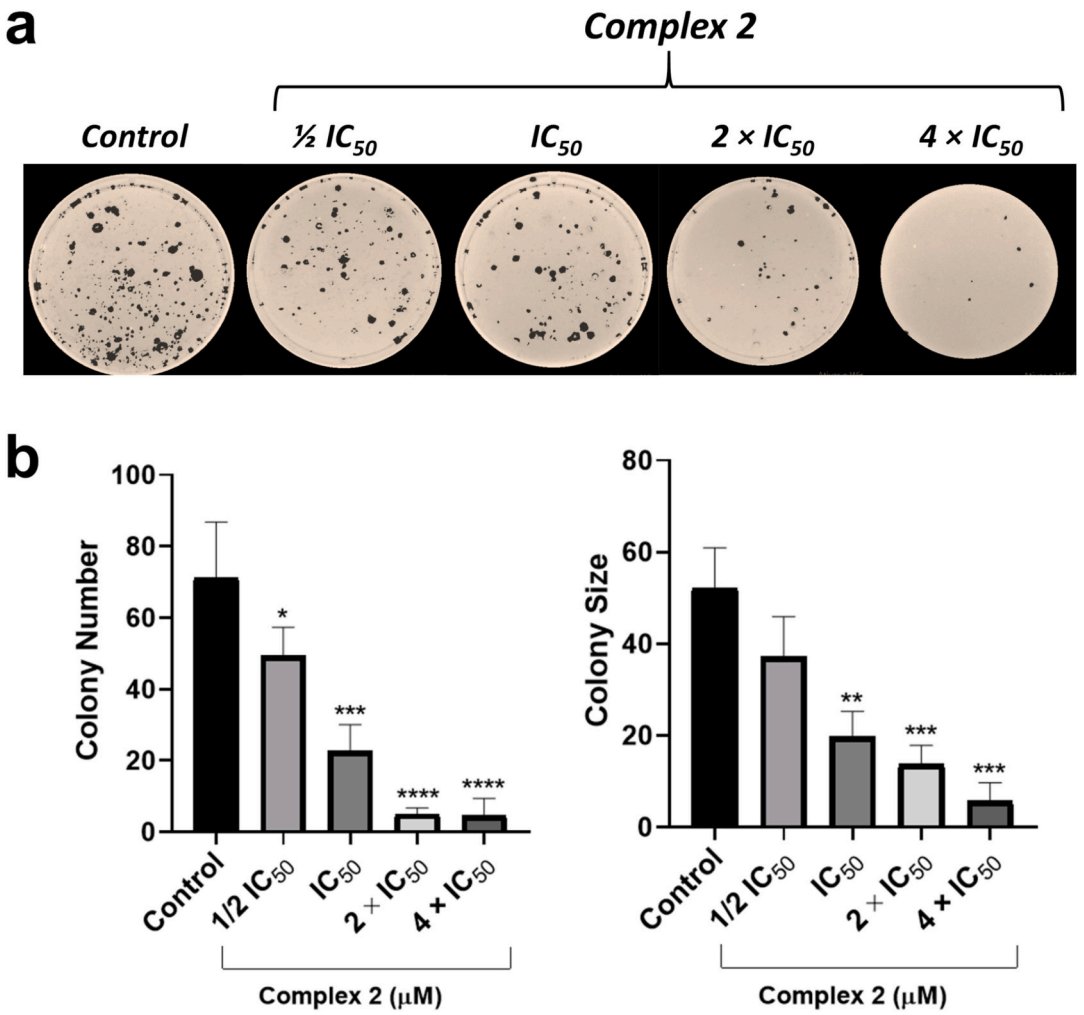

Fig. 4. Effects of compound **2** on colony formation. (a) Assessment of the cell survival by clonogenic assay. Representative colony formation images of A2780 cells after treatment with different concentrations of **2**. A representative image from one of the triplicates is shown. (b) Quantitative data representing the colony number and area with relation to the concentration of **2**. DMSO was employed as negative control (0.5 %). Data are expressed as mean ± SD of three independent measurements. The statistical analysis was performed with one-way ANOVA test (*$p < 0.05$; **$p < 0.01$; ***$p < 0.001$ and ****$p < 0.0001$).

Thus, A2780 cells were treated with different concentrations of the compound, and the colonies formed after 10 days were colored with violet-blue, washed and dried. The results presented in Fig. 4a revealed a decrease on the cell survival upon treatment with **2** at 0.05 μM (½ IC_{50} concentration). The number and the area of the colonies were drastically reduced with the increasing the concentration, thus revealing both cytotoxic and cytostatic activities of **2** (Fig. 4b). This behavior has been reported for similar Ru-phosphine compounds on different cell lines [17,22].

3.4. MCTS growth inhibition

After evaluation of the cytotoxicity on 2D monolayer cells, the effect of **2** was studied on multicellular tumor spheroids (MCTS). The 3D approach presents advantages compared to conventional 2D assays. MCTS are cell aggregates that simulate the gradient of nutrients and oxygen, mimicking the *in vivo* tumor environment [33–35]. In this experiment, the spheroids were incubated for 6 days upon the treatment with the ruthenium(II) compound at different concentrations. As shown in Fig. 5a and b, **2** inhibited the spheroid growth at 0.4 μM, leading to a decrease in tumor volume after 48 h of treatment. It is worth mentioning that the cell death was triggered in 3D MCTS only in concentrations higher than observed in the 2D assay, as observed for other Ru(II)-based compounds [36]. Further, to obtain more insights regarding the cell damage, DAPI/PI dual staining assay was performed after day 6 (Fig. 5c). The images reveal a similar profile for **2** in a concentration range from 0.4 to 10 μM, which is reinforced by the intensification of PI colour, confirming the cell death.

3.5. Mechanism of action

A series of targeted biological experiments were performed to gain a deeper understanding of the mechanism of action of compound **2**. First, cell cycle analysis distribution was assessed by flow cytometry. As presented in Fig. 6, most of the untreated cells were found at the G1 phase of the cell cycle (~ 62 %) (Fig. 6a). The effect of compound **2** is only observed at concentrations higher than IC_{50}, where it can see a change in cell cycle distribution due to an increase of cells at the G1 phase. It should be mentioned compound **2** probably acts differently from cisplatin since studies have reported that this drug promotes the arrest of the S phase in ovarian A2780 cancer cell [37].

In the second part of our investigation, we decided to study the mitochondrial membrane potential (MMP, $\Delta\psi m$) of these cells. As mentioned, some Ru-based compounds are able to affect the mitochondrial membrane and this behavior is typical of apoptotic cell death [41]. For this, we monitored the JC-1 fluorescence upon its accumulation in the healthy/damaged mitochondria. JC-1 is cyanine dye that can be used as a sensitive MMP indicator.

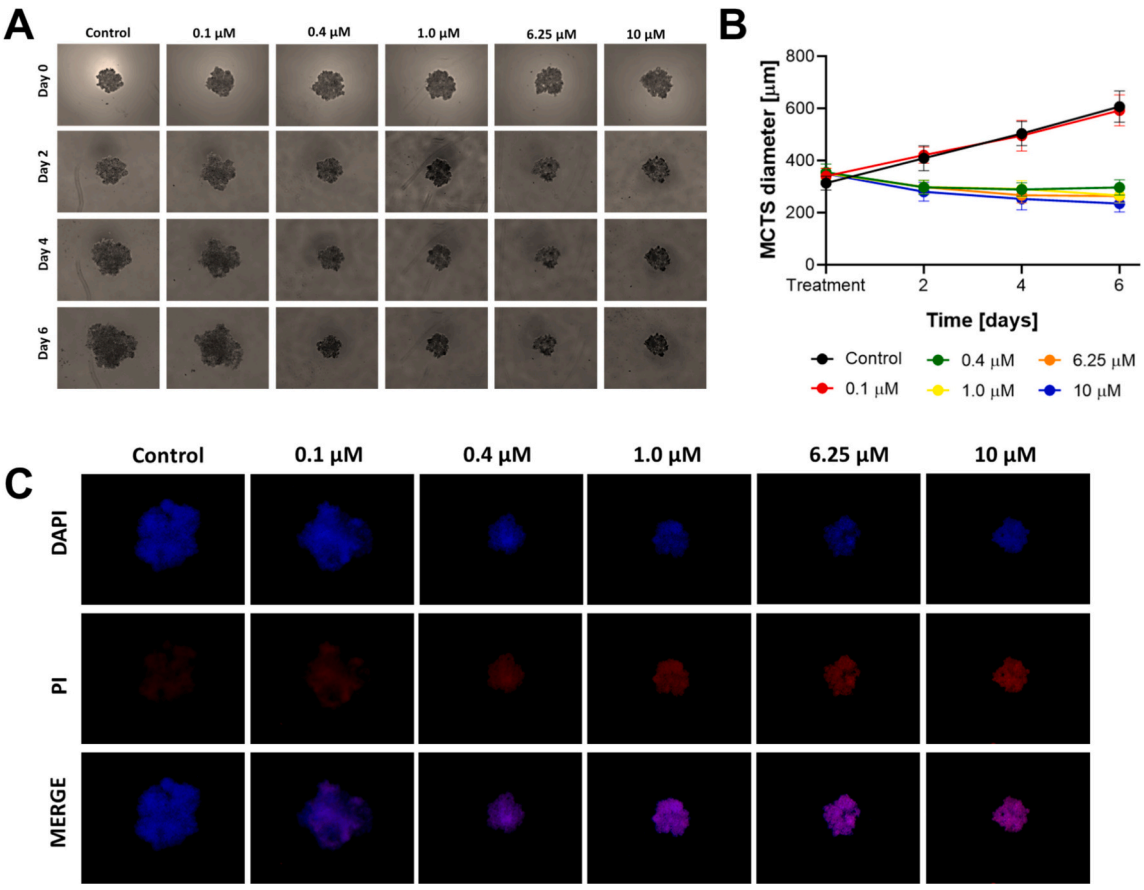

Fig. 5. Changes in the growth kinetics of MCTSs treated with **2** at different concentrations (0.1, 0.4, 1.0, 6.25, and 10 μM). (a) Images were collected on day 0 (before treatment) and days 2, 4, and 6. (b) MCTS diameter was measured at different time points. (c) DAPI/PI MCTS staining after day 6.

When accumulated in a healthy mitochondria (higher membrane potential), JC-1 forms red-fluorescent aggregates, emits fluorescence at 590 nm (red). In the other hand, if a mitochondrial damage is detected (higher membrane potential), JC-1changes to a monomeric form, emitting fluorescence at 530 nm (green) (Fig. 6b). Fig. 6c shows the ratio red-to-green JC-1 fluorescence before and after treatment with **2**. As expected, a red fluorescence is observed in the absence of the ruthenium compound, revealing JC-1 in an aggregate form. However, after the treatment, a decrease on the signal is detected, indicating a mitochondrial damage, which is an event of apoptosis [38,41].

As Δψm decreasing is a process related to apoptotic damage, this cell death process was further studied by flow cytometry using 7-AAD (7-Aminoactinomycin D) and annexin V staining. While 7-AAD can penetrate into cell membranes of dead or damaged cells, anexin V binds to the membrane phospholipid phosphatidylserine (PS) that is exposed in apoptotic cells. For the experiments, A2780 cells were treated with compound **2** at different concentrations and the cells were categorized as viable, early apoptosis, late apoptosis, and necrosis. As presented in Fig. 7a, in the control (CTRL) most of ovarian cells were viable (96.3 %), indicating the absence of apoptotic cells. On the other hand, a remarkable change was verified after addition of **2** at concentrations lower than IC_{50}. As shown, the total of cells undergoing to the apoptotic process (early apoptosis + late apoptosis) is 29.8 %. Curiously, at the highest concentration tested (4 × IC_{50}), the total of apoptotic cells was 40.4 %, indicating that this slight increase in the apoptosis process had no direct correlation with the concentration of Ru(II) compound.

To reinforce these findings, cell images using fluorescence microscopy were taken in a presence of **2** at 0.40 μM (4 × IC_{50} concentration). Then, DAPI and PI fluorescent dyes were added and the images were captured after additional 1 h incubation. The fluorescence intensity was monitored by imaging using an excitation wavelength for DAPI and PI coupled in a CELENA® S Digital Imaging System. As observed in Fig. 7b, the co-localization of DAPI and PI was determined. Different from DAPI internalization, PI is selective for cells undergoing to apoptosis, which is represented by condensed and fragmented chromatin. Our results qualitatively confirm the cell death caused by **2**, which is in agreement with flow cytometry results.

3.6. P53, PCNA, γH2AX and cleaved caspase 3 expression

Fig. 8 presents the results obtained from the analysis of the levels of proteins p53, PCNA, γH2AX, and cleaved caspase-3 in A2780 cancer cell after treatment with **2** at IC_{50} and 2 x IC_{50} concentrations. The results demonstrate an increase in the expression levels of p53, an important marker for cell cycle control, DNA repair, and apoptosis induction, in both concentrations tested. The expression levels of PCNA, a cell proliferation marker, decreased significantly with both concentrations of **2**. In the other hand the expression levels of γH2AX and cleaved caspase-3, markers of double-strand DNA damage and apoptosis, respectively, increased in the presence of **2**, in a concentration-dependent manner. These findings suggest that treatment with Ru at both concentrations induces A2780 cell death by apoptosis, likely due to double-strand DNA damage and failure in cellular repair mechanisms, in accordance with our flow cytometry results.

These findings suggest that **2**, under these experimental conditions, interacts with DNA, causing damage to the genetic material of tumor cells, leading to increased expression of p53 and, therefore, acts on the cell cycle, leading to the induction of apoptosis, which is observed by increased levels of cleaved caspase 3 [39,40]. Thus, the modulation of this pathway significantly reduced the proliferation of cancer cells,

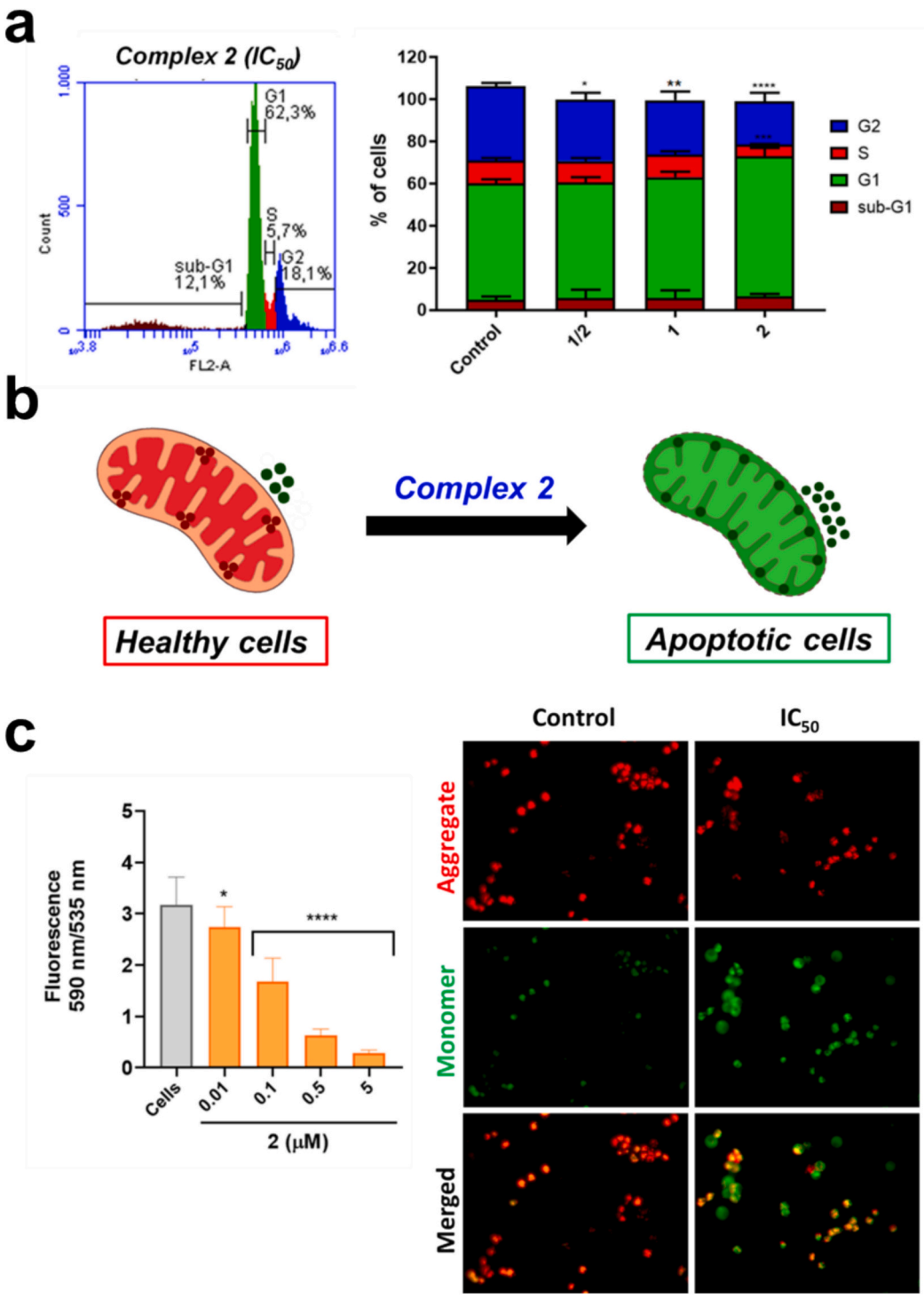

Fig. 6. (a) Cell cycle distribution on A2780 cells and the relative expression of percentage of cells in each phase after treatment with complex **2** during 48 h. (b) Schematic diagram depicting the presence of JC-1 aggregates (red; healthy cells) and JC-1 monomers (green; apoptotic cells) as a result of treatment with **2**. * $p < 0.05$; ** $p < 0.01$ and **** $p < 0.0001$. (c) Mitochondrial membrane potential (MMP) test: (left) fluorescence signal of the JC-1 dye detected in A2780 cells treated for 24 h with different concentrations of **2** (from 0.01 to 5 μM). DMSO (1 %) was used as negative control. The signal was obtained using the aggregate/monomer ratios, (right) fluorescence microscope analysis of MMP level by JC-1 staining after complex **2** treatment for 24 h. (For interpretation of the references to colour in this figure legend, the reader is referred to the web version of this article.)

resulting in a decrease in PCNA expression.

4. Conclusion

We studied the anticancer potential of three ruthenium(II)-diphosphine complexes (**1**–**3**) against ovarian cancer cells. Complex $[Ru(mmi)(dppe)_2]PF_6$ (**2**) showed a better performance against A2780 cells, with IC_{50} values equal to 0.11 μM and higher selectivity than cisplatin control. This complex affects the morphology and colony formation in these cells, exhibiting both cytotoxic and cytostatic effects. Flow cytometry and fluorescence microscopy revealed that **2** acts *via* an apoptotic pathway changing the mitochondrial membrane potential.

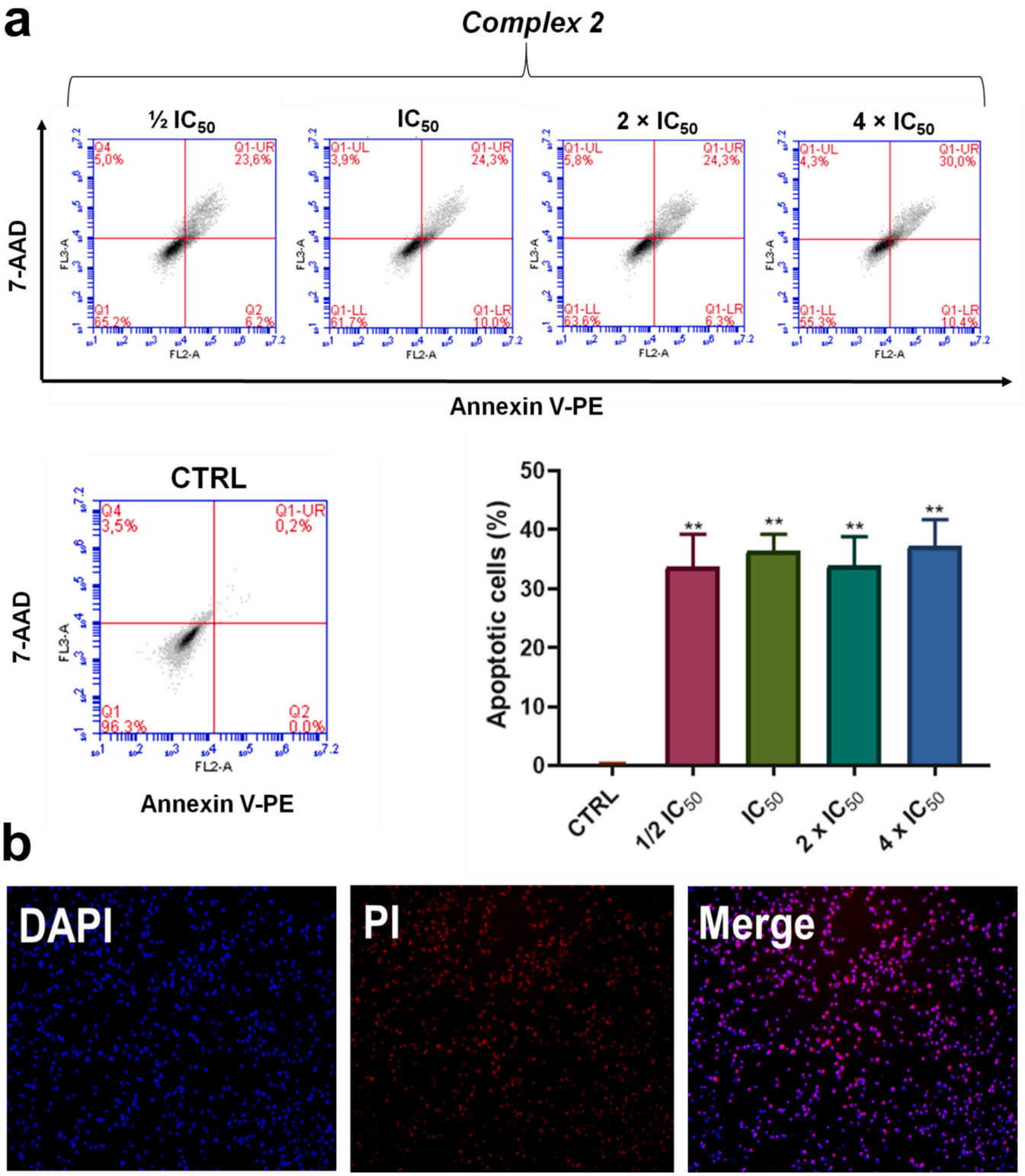

Fig. 7. (a) Induction of apoptosis in A2780 cells and quantification of the cells undergoing to late apoptosis after treatment with **2** for 24 h. The statistical analysis was one-way ANOVA followed by Tukey's comparison test. $^{**}p < 0.01$. (b) DAPI/PI staining A2780 cells treated with **2** ($2 \times IC_{50}$).

Furthermore, western blotting results demonstrated that p53, PCNA, γH2AX and cleaved caspase 3 had their levels altered upon treatment with **2**, indicating a double-strand DNA damage followed by a failure in cellular repair mechanisms. Taken together, the results encourage further studies with this complex and point to it as a promising anti-cancer agent against ovarian cancer, which is still limited.

CRediT authorship contribution statement

Marcos V. Palmeira-Mello: Investigation, Methodology, Validation, Data curation, Conceptualization, Writing – original draft. **Tamara Teixeira:** Investigation. **Matheus Reis Santos de Melo:** Investigation. **Heloiza Diniz Nicolella:** Investigation. **Jocely L. Dutra:** Investigation. **Marcia R. Cominetti:** Resources, Writing – review & editing. **Fillipe**

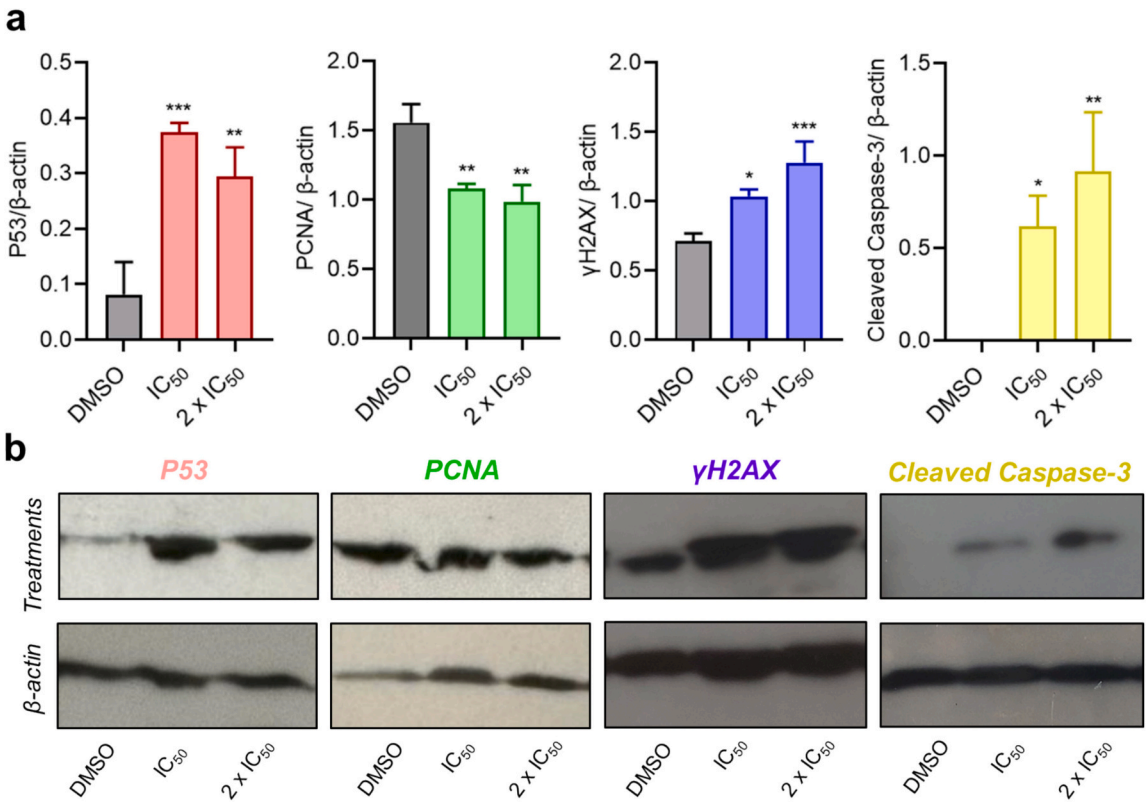

Fig. 8. Western blotting analysis on A2780 human ovarian cancer cells after 24 h of treatment with **2** at IC_{50} and 2 x IC_{50} concentrations. (a) Expression of p53, PCNA, γH2AX and Cleaved Caspase-3. (b) Photography of developing films. Data are expressed as mean ± SD. The statistical analysis was one-way ANOVA followed by Tukey's comparison test (* $p < 0.05$; ** $p < 0.01$ and *** $p < 0.001$).

Vieira Rocha: Resources, Funding acquisition, Supervision, Writing – review & editing. **Denise Crispim Tavares:** Resources, Funding acquisition, Supervision, Writing – review & editing. **Alzir A. Batista:** Conceptualization, Funding acquisition, Supervision, Writing – review & editing.

Declaration of competing interest

The authors declare that they have no known competing financial interests or personal relationships that could have appeared to influence the work reported in this paper.

Data availability

Data will be made available on request.

Acknowledgements

We thank the São Paulo State Research Support Foundation (FAPESP, Grants 2023/02475-8 and 2022/02876-0) and CNPq for financial support. M.V.P.-M. thanks FAPESP for a postdoctoral fellowship (Grant 2021/01787-0). This study was financed in part by Coordenação de Aperfeiçoamento de Pessoal de Nível Superior – Brazil (CAPES) – Finance Code 001. We thank MSc. Carlos André F. Moraes (UFSCar, Brazil) for the mass spectrometry experiments.

Appendix A. Supplementary data

Supplementary data to this article can be found online at https://doi.org/10.1016/j.jinorgbio.2024.112819.

References

[1] American Cancer Society. https://www.cancer.org/cancer/types/ovarian-cancer, 2024 accessed on July, 2024.
[2] B.A. Chabner, T.G. Roberts, Nat. Rev. Cancer 5 (2005) 65–72, https://doi.org/10.1038/nrc1529.
[3] L. Kelland, Nat. Rev. Cancer 7 (2007) 573–584, https://doi.org/10.1038/nrc2167.
[4] S. Rottenberg, C. Disler, P. Perego, Nat. Rev. Cancer 21 (1) (2020) 37–50, https://doi.org/10.1038/s41568-020-00308-y.
[5] R. Oun, Y.E. Moussa, N.J. Wheate, Dalton Trans. 47 (19) (2018) 6645–6653, https://doi.org/10.1039/c8dt00838h.
[6] J. Zhou, Y. Kang, L. Chen, H. Wang, J. Liu, S. Zeng, L. Yu, Front. Pharmacol. 11 (2020) 343, https://doi.org/10.3389/fphar.2020.00343.
[7] C. Marchetti, F. De Felice, A. Romito, V. Iacobelli, C.M. Sassu, G. Corrado, C. Ricci, G. Scambia, A. Fagotti, Semin. Cancer Biol. 77 (2021) 144–166, https://doi.org/10.1016/j.semcancer.2021.08.011.
[8] S.Y. Lee, C.Y. Kim, T.G. Nam, Drug Des. Devel. Ther. 14 (2020) 5375–5392, https://doi.org/10.2147/dddt.s275007.
[9] Pragti, B.K. Kundu, S. Mukhopadhyay, Coord. Chem. Rev. 448 (2021) 214169, https://doi.org/10.1016/j.ccr.2021.214169.
[10] G.H. Ribeiro, A.R. Costa, A.R. de Souza, F.V. da Silva, F.T. Martins, A.M. Plutin, A. A. Batista, Coord. Chem. Rev. 488 (2023) 215161, https://doi.org/10.1016/j.ccr.2023.215161.
[11] S. Thota, D.A. Rodrigues, D.C. Crans, E.J. Barreiro, J. Med. Chem. 61 (14) (2018) 5805–5821, https://doi.org/10.1021/acs.jmedchem.7b01689.
[12] K.J. Franz, N. Metzler-Nolte, Chem. Rev. 119 (2019) 727–729, https://doi.org/10.1021/acs.chemrev.8b00685.
[13] E. Boros, P.J. Dyson, G. Gasser, Chem 6 (2020) 41–60, https://doi.org/10.1016/j.chempr.2019.10.013.
[14] C.G. Hartinger, M.A. Jakupec, S. Zorbas-Seifried, M. Groessl, A. Egger, W. Berger, H. Zorbas, P.J. Dyson, B.K. Keppler, Chem. Biodivers. 5 (2008) 2140–2155, https://doi.org/10.1002/cbdv.200890195.
[15] E. Alessio, G. Mestroni, A. Bergamo, G. Sava, Curr. Top. Med. Chem. 4 (15) (2004) 1525–1535, https://doi.org/10.2174/1568026043387421.
[16] E.R. dos Santos, M.A. Mondelli, L.V. Pozzi, R.S. Correa, H.S. Salistre-de-Araujo, F. R. Pavan, C.Q.F. Leite, J. Ellena, V.R.S. Malta, S.P. Machado, A.A. Batista, Polyhedron 51 (2013) 292–297, https://doi.org/10.1016/j.poly.2013.01.004.
[17] G.H. Ribeiro, A.P.M. Guedes, T.D. de Oliveira, C.R.S.T.B. de Correia, L. Colina-Vegas, M.A. Lima, J.A. Nóbrega, M.R. Cominetti, F.V. Rocha, A.G. Ferreira, E. E. Castellano, F.R. Teixeira, A.A. Batista, Inorg. Chem. 59 (2020) 15004–15018, https://doi.org/10.1021/acs.inorgchem.0c01835.

[18] K.M. Oliveira, E.J. Peterson, M.C. Carroccia, M.R. Cominetti, V.M. Deflon, N. P. Farrell, A.A. Batista, R.S. Correa, Dalton Trans. 49 (45) (2020) 16193–16203, https://doi.org/10.1039/d0dt01091j.
[19] K.M. Oliveira, J. Honorato, F.C. Demidoff, M.S. Schultz, C.D. Netto, M. R. Cominetti, R.S. Correa, A.A. Batista, J. Inorg. Biochem. 214 (2021) 111289, https://doi.org/10.1016/j.jinorgbio.2020.111289.
[20] V.S. Velozo-Sá, L.R. Pereira, A.P. Lima, F. Mello-Andrade, M.R.M. Rezende, R. M. Goveia, W.C. Pires, M.M. Silva, K.M. Oliveira, A.G. Ferreira, J. Ellena, V. M. Deflon, C.K. Grisolia, A.A. Batista, E.P. Silveira-Lacerda, Dalton Trans. 48 (18) (2019) 6026–6039, https://doi.org/10.1039/c8dt03738h.
[21] B.N. Cunha, L. Colina-Vegas, A.M. Plutín, R.G. Silveira, J. Honorato, K.M. Oliveira, M.R. Cominetti, A.G. Ferreira, E.E. Castellano, A.A. Batista, J. Inorg. Biochem. 186 (2018) 147–156, https://doi.org/10.1016/j.jinorgbio.2018.06.007.
[22] M.V. Palmeira-Mello, A.R. Costa, L.P. de Oliveira, O. Blacque, G. Gasser, A. A. Batista, Dalton Trans. 53 (2024) 10947–10960, https://doi.org/10.1039/D4DT01191K.
[23] J. Cervinka, A. Gobbo, L. Biancalana, L. Markova, V. Novohradsky, M. Guelfi, S. Zacchini, J. Kasparkova, V. Brabec, F. Marchetti, J. Med. Chem. 65 (15) (2022) 10567–10587, https://doi.org/10.1021/acs.jmedchem.2c00722.
[24] R.J. Mitchell, A.S. Gowda, A.G. Olivelli, A.J. Huckaba, S. Parkin, J.M. Unrine, V. Oza, J.S. Blackburn, F. Ladipo, D.K. Heidary, E.C. Glazer, Inorg. Chem. 62 (28) (2023) 10940–10954, https://doi.org/10.1021/acs.inorgchem.3c00736.
[25] M.M. da Silva, G.H. Ribeiro, M.S. de Camargo, A.G. Ferreira, L. Ribeiro, M.I. F. Barbosa, V.M. Deflon, S. Castelli, A. Desideri, R.S. Corrêa, A.B. Ribeiro, H. D. Nicolella, S.D. Ozelin, D.C. Tavares, A.A. Batista, Inorg. Chem. 60 (2021) 14174–14189, https://doi.org/10.1021/acs.inorgchem.1c01539.
[26] T. Mosmann, J. Immunol. Methods 65 (1983) 55–63, https://doi.org/10.1016/0022-1759(83)90303-4.
[27] A.B. Ribeiro, H.D. Nicolella, L.H.D. da Silva, J.A.A. Mejía, M.H. Tanimoto, S. R. Ambrósio, J.K. Bastos, R.P. Orenha, R.L.T. Parreira, D.C. Tavares, Planta Med. 89 (2023) 158–167, https://doi.org/10.1055/a-1890-5446.
[28] M.M. da Silva, M.S. de Camargo, R.S. Correa, S. Castelli, R.A. De Grandis, J. E. Takarada, E.A. Varanda, E.E. Castellano, V.M. Deflon, M.R. Cominetti, A. Desideri, A.A. Batista, Dalton Trans. 48 (2019) 14885, https://doi.org/10.1039/c9dt01905g.
[29] J. Grau, A. Caubet, O. Roubeau, D. Montpeyó, J. Lorenzo, P. Gamez, ChemBioChem 21 (16) (2020) 2348–2355, https://doi.org/10.1002/cbic.202000154.
[30] J.M.S. Cardoso, I. Correia, A.M. Galvão, F. Marques, M.F.N.N. Carvalho, J. Inorg. Biochem. 166 (2017) 55–63, https://doi.org/10.1016/j.jinorgbio.2016.11.003.
[31] D. Wlodkowic, W. Telford, J. Skommer, Z. Darzynkiewicz, Methods Cell Biol. 103 (2011) 55–98, https://doi.org/10.1016/B978-0-12-385493-3.00004-8.
[32] H. Rafehi, C. Orlowski, G.T. Georgiadis, K. Ververis, A. El-Osta, T.C. Karagiannis, J. Vis. Exp. 49 (2011) e2573, https://doi.org/10.3791/2573.
[33] J.S. Joseph, S.T. Malindisa, M. Ntwasa, Cell Culture, 2018, https://doi.org/10.5772/intechopen.81552.
[34] M.C. Ruiz, J. Kljun, I. Turel, A.L. Di Virgilio, I.E. León, Metallomics 11 (3) (2019) 666–675, https://doi.org/10.1039/c8mt00369f.
[35] R.A. De Grandis, P.W.S. dos Santos, K.M. de Oliveira, A.R.T. Machado, A.F. Aissa, A.A. Batista, L.M.G. Antunes, F.R. Pavan, Bioorg. Chem. 85 (2019) 455–468, https://doi.org/10.1016/j.bioorg.2019.02.010.
[36] J. Karges, F. Heinemann, M. Jakubaszek, F. Maschietto, C. Subecz, M. Dotou, R. Vinck, O. Blacque, M. Tharaud, B. Goud, E.V. Zahínos, B. Spingler, I. Ciofini, G. Gasser, J. Am. Chem. Soc. 142 (2020) 6578–6587, https://doi.org/10.1021/jacs.9b13620.
[37] M. Kielbik, D. Krzyzanowski, B. Pawlik, M. Klink, Oncotarget 9 (28) (2018) 19847–19860, https://doi.org/10.18632/oncotarget.24884.
[38] Z. Zhu, Z. Wang, C. Zhang, Y. Wang, H. Zhang, Z. Gan, Z. Guo, X. Wang, Chem. Sci. 10 (2019) 3089, https://doi.org/10.1039/c8sc04871a.
[39] M.R.S. de Melo, A.B. Ribeiro, G. Fernandes, I.S. Squarisi, M.M. Junqueira, A. A. Batista, M.M. da Silva, D.C. Tavares, J. Biol. Inorg. Chem. 29 (2024) 159–168, https://doi.org/10.1007/s00775-023-02036-8.
[40] V.R. Silva, R.S. Corrêa, L.S. Santos, M.B.P. Soares, A.A. Batista, D.P. Bezerra, Sci. Rep. 8 (2018) 288, https://doi.org/10.1038/s41598-017-18639-6.
[41] M.V. Palmeira-Mello, P. Mesdom, P. Burckel, S. Hidalgo, O. Blacque, G. Gasser, A. A. Batista, ChemBioChem (2025), https://doi.org/10.1002/cbic.202400734.